Mon. Not. R. Astron. Soc. **393,** 491–500 (2009) doi:10.1111/j.1365-2966.2008.14009.x

Two-component galaxies with flat rotation curve

Luca Ciotti,[1]★ Lucia Morganti[1]† and P. T. de Zeeuw[2,3]

[1]*Astronomy Department, University of Bologna, via Ranzani 1, 40127 Bologna, Italy*
[2]*Leiden Observatory, Leiden University, PO Box 9513, 2300 RA Leiden, The Netherlands*
[3]*ESO, Karl Schwarzschildstrasse 2, 85748 Garching bei Muenchen, Germany*

Accepted 2008 September 25. Received 2008 September 24; in original form 2008 August 9

ABSTRACT

Dynamical properties of two-component galaxy models whose stellar density distribution is described by a γ model while the total density distribution has a pure r^{-2} profile are presented. The orbital structure of the stellar component is described by Osipkov–Merritt anisotropy, while the dark matter halo is isotropic. After a description of minimum halo models, the positivity of the phase-space density (the model consistency) is investigated, and necessary and sufficient conditions for consistency are obtained analytically as a function of the stellar inner density slope γ and anisotropy radius. The explicit phase-space distribution function is recovered for integer values of γ, and it is shown that while models with $\gamma > 4/17$ are consistent when the anisotropy radius is larger than a critical value (dependent on γ), the $\gamma = 0$ models are unphysical even in the fully isotropic case. The Jeans equations for the stellar component are then solved analytically; in addition, the projected velocity dispersion at the centre and at large radii are also obtained analytically for generic values of the anisotropy radius, and it is found that they are given by remarkably simple expressions. The presented models, even though highly idealized, can be useful as starting point for more advanced modelling of the mass distribution of elliptical galaxies in studies combining stellar dynamics and gravitational lensing.

Key words: stellar dynamics – celestial mechanics – galaxies: kinematics and dynamics.

1 INTRODUCTION

Analysis of stellar kinematics (e.g. Bertin et al. 1994b; Rix et al. 1997; Gerhard et al. 2001), as well as several studies combining stellar dynamics and gravitational lensing, strongly support the idea that the dark and the stellar matter in elliptical galaxies are distributed so that their total mass profile is described by a density distribution proportional to r^{-2} (e.g. see Treu & Koopmans 2002, 2004; Rusin, Kochanek & Keeton 2003; Rusin & Kochanek 2005; Koopmans et al. 2006; Czoske et al. 2008; Dye et al. 2008). In particular, Gavazzi et al. (2007), with a gravitational lensing analysis of 22 early-type strong lens galaxies, reported a total r^{-2} density profile in the range 1–100 effective radii. It is clear that in this field the availability of simple dynamical models of two-component galaxies can be useful as starting point of more sophisticated investigations based on axisymmetric or triaxial galaxy models (e.g. Cappellari et al. 2007; van den Bosch et al. 2008). A few simple yet interesting models with flat rotation curve have been in fact constructed, such as those in which the stellar mass was described by a power law in a total r^{-2} mass distribution (e.g. Kochanek 1994), or those obtained from physical arguments (in case of disc galaxies, see e.g. Naab & Ostriker 2007).

Here the family of two-component galaxy models whose total mass density is proportional to r^{-2}, while the visible (stellar) mass is described by the well known γ models (Dehnen 1993; Tremaine et al. 1994), is presented. Some preliminary numerical investigation of these models has been done in Keeton (2001), and they have been used in Nipoti, Treu & Bolton (2008) as diagnostics of the total mass distribution in elliptical galaxies (see also Thomas et al. 2007). In this paper a more systematic study of the dynamical properties of these models is presented. It is shown that the Jeans equations for the stellar component with Osipkov–Merritt (OM; Osipkov 1979; Merritt 1985) radial anisotropy can be solved analytically. Remarkably, the projected velocity dispersion at the centre and at large radii can be expressed in terms of the model circular velocity by means of extremely simple formulae for generic values of the anisotropy radius and of the central stellar density slope γ. In principle this feature opens the possibility to obtain preliminary indications about the anisotropy from observations at small and large radii. The positivity of the phase-space density (the so-called consistency) is investigated, by obtaining analytically the necessary and sufficient conditions for model consistency in terms of γ, of the anisotropy radius, and of the dark-to-stellar mass ratio within some prescribed radius. It is found that the phase-space distribution function (DF) can be recovered analytically for $\gamma = 0$, 1 and 2. In particular, it is shown

★E-mail: luca.ciotti@unibo.it
†Present address: Max-Planck-Institut für Ex. Physik, Giessenbachstraße, D-85741 Garching, Germany.

© 2009 The Authors. Journal compilation © 2009 RAS

that $\gamma = 0$ models in a total r^{-2} density profile are unphysical for any value of the anisotropy radius. These results extend the class of two-component galaxy models with explicit DF and add to the large amount of phase-space information already available about one- and two-component γ models (e.g. see Dehnen 1993; Hiotelis 1994; Tremaine et al. 1994; Carollo, de Zeeuw & van der Marel 1995; Ciotti 1996, hereafter C96; Ciotti 1999, hereafter C99; Baes, Dejonghe & Buyle 2005; Buyle, Hunter & Dejonghe 2007; Ciotti & Morganti 2008).

The paper is organized as follows. In Section 2 the main structural properties of the models are presented, while in Section 3 an investigation of the phase-space properties of the models is carried out both from the point of view of necessary and sufficient conditions for consistency and of direct recovery of the DF in specific cases. In Section 4 the solution of the Jeans equation with OM radial anisotropy is presented, together with their projection at small and large radii. Finally, a short summary of possible use of the present models in observational works is given.

2 THE MODELS

2.1 Stellar distribution

The density profile of spherical γ models is

$$\rho_*(r) = \frac{A_*}{s^\gamma (1+s)^{4-\gamma}}, \qquad A_* \equiv \frac{(3-\gamma)M_*}{4\pi {r_*}^3}, \tag{1}$$

where $0 \le \gamma < 3$, M_* is the total stellar mass, r_* is a scalelength and $s \equiv r/r_*$ is the dimensionless radius. These models have been investigated extensively, and here only the properties of present use are listed. In particular, the cumulative stellar mass within r is given by

$$M_*(r) = M_* \left(\frac{s}{1+s}\right)^{3-\gamma}, \tag{2}$$

so that the dimensionless half-mass spatial radius is $s_\mathrm{h} = 1/[2^{1/(3-\gamma)} - 1]$. The projected stellar surface density

$$\Sigma_*(R) = 2\int_R^\infty \frac{\rho_*(r) r\, \mathrm{d}r}{\sqrt{r^2 - R^2}} \tag{3}$$

(e.g. Binney & Tremaine 2008) cannot be expressed in terms of elementary functions for generic values of γ; however, the asymptotic behaviour of $\Sigma_*(R)$ is easily obtained for $R \to 0$,

$$\Sigma_*(R) \sim A_* r_* \begin{cases} \dfrac{4}{(3-\gamma)(2-\gamma)(1-\gamma)}, & (0 \le \gamma < 1), \\ -2\log\eta, & (\gamma = 1), \\ \dfrac{\sqrt{\pi}\,\Gamma(\gamma/2 - 1/2)}{\Gamma(\gamma/2)} \eta^{1-\gamma}, & (1 < \gamma \le 3), \end{cases} \tag{4}$$

and for $R \to \infty$,

$$\Sigma_*(R) \sim \frac{\pi A_* r_*}{2\eta^3}, \quad (0 \le \gamma \le 3). \tag{5}$$

In the equations above R is the radius on the projection plane, $\eta \equiv R/r_*$ is its normalized value and Γ is the complete Euler gamma function; note that the first of equation (4) is the exact value of the projection integral for $R = 0$ when $0 \le \gamma < 1$.

2.2 Total and dark matter distribution

By assumption the total mass density is taken to be

$$\rho_\mathrm{T}(r) = \frac{\mathcal{R} A_*}{s^2}, \tag{6}$$

where $\mathcal{R}$ is a dimensionless scalefactor which measures the importance of the dark matter density with respect to the stellar one; therefore, the stellar distribution would be a tracer in the total density distribution in the formal limit $A_* \to 0$ and $\mathcal{R} \to \infty$, in a way such that the product $\mathcal{R}A_*$ remains constant. The cumulative total mass within r is

$$M_\mathrm{T}(r) = 4\pi \mathcal{R} A_* r_*^3 s, \tag{7}$$

and the system (constant) circular velocity is $v_\mathrm{c}^2 = 4\pi G \mathcal{R} A_* r_*^2$; from this expression the dimensionless constant $\mathcal{R}$ (or the density scale A_*) everywhere appears in favour of v_c. The total projected mass density at R is obtained from equations (3) and (6) as

$$\Sigma_\mathrm{T}(R) = \frac{\pi \mathcal{R} A_* r_*}{\eta}, \tag{8}$$

so that the total mass contained within the cylinder of radius R is

$$M_\mathrm{PT}(R) = 2\pi \int_0^R \Sigma_\mathrm{T}(R)\, R\, \mathrm{d}R = 2\pi^2 \mathcal{R} A_* r_*^3 \eta. \tag{9}$$

Not all values of the coefficient $\mathcal{R}$ and of the inner stellar density slope γ are compatible. In fact a first limitation is given by the request of positivity for the halo density

$$\rho_\mathrm{h}(r) = \frac{A_*}{s^2}\left[\mathcal{R} - \frac{s^{2-\gamma}}{(1+s)^{4-\gamma}}\right]. \tag{10}$$

This request restricts the value of γ to the interval $0 \le \gamma \le 2$, independently of the value of $\mathcal{R}$. With γ in the acceptable range, ρ_h is positive provided that

$$\mathcal{R} \ge \mathcal{R}_\mathrm{m}(\gamma) = \frac{4(2-\gamma)^{2-\gamma}}{(4-\gamma)^{4-\gamma}} \tag{11}$$

(see Appendix A). For example, $\mathcal{R}_\mathrm{m}(0) = 1/16$, $\mathcal{R}_\mathrm{m}(1/2) = 0.0916$, $\mathcal{R}_\mathrm{m}(1) = 4/27$ and $\mathcal{R}_\mathrm{m}(2) = 1$; in Fig. 1 (bottom panel) the minimum value $\mathcal{R}_\mathrm{m}(\gamma)$ for halo positivity is represented by the solid line. A dark halo with $\mathcal{R}_\mathrm{m}$ is called a minimum halo. While the density distribution of the minimum halo increases at the centre as r^{-2} for $0 \le \gamma < 2$, for $\gamma = 2$ it results $\rho_\mathrm{h} \propto r^{-1}$, and so minimum halo $\gamma = 2$ models are more and more baryon dominated near the centre. We remark that the local mass-to-light ratio, proportional to $\rho_\mathrm{T}(r)/\rho_*(r)$ under the hypothesis of a constant stellar mass-to-light ratio, is a non-monotonic function of r as it increases near the centre and for $r \to \infty$. The only exception is represented by the $\gamma = 2$ case, which is characterized by a monotonically increasing mass-to-light ratio for increasing r.

Of course, the positivity of ρ_h is just a first condition for the acceptability of the model. A plausible second request is the monotonicity of ρ_h as a function of radius, while at this stage monotonicity reduces to the determination of a minimum value of $\mathcal{R}_\mathrm{m}(\gamma)$ so that $\mathrm{d}\rho_\mathrm{h}/\mathrm{d}r \le 0$, in Section 3 it will be shown that this request is based on deeper physical arguments than simple structural plausibility. The explicit calculation of this additional restriction of $\mathcal{R}$ is given in Appendix A, and the resulting function $\mathcal{R}_\mathrm{m}(\gamma)$ is shown in Fig. 1 (bottom panel) with the dotted line; it is apparent that the request of monotonicity is just a little bit more stringent than positivity, and that in the $\gamma = 2$ case the two requests coincide.

It can be of interest in applications to evaluate the relative amount of dark to visible mass within a prescribed radius. This quantity is easily calculated from equations (2) and (7). For example, within the half-mass radius r_h one has

$$\frac{M_\mathrm{h}(r_\mathrm{h})}{M_*(r_\mathrm{h})} \ge \frac{2(3-\gamma)\mathcal{R}_\mathrm{m}(\gamma)}{2^{1/(3-\gamma)} - 1} - 1, \tag{12}$$

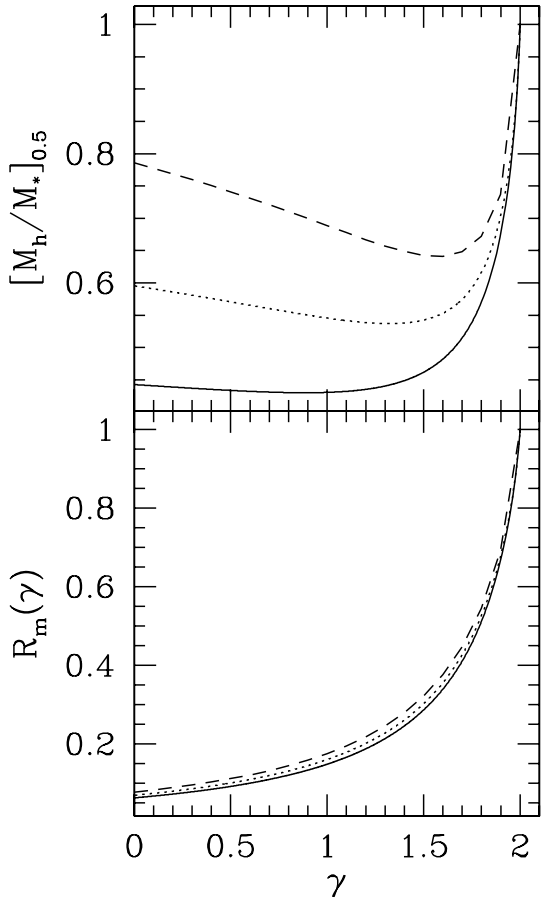

Figure 1. Bottom panel: minimum value of $\mathcal{R}$ as a function of γ for the halo density positivity (solid line, equation 11), monotonicity (dotted line, equation A2) and to satisfy the WSC in the isotropic case (dashed line, equations 18–A4). Top panel: the dark to stellar mass ratio within the half-mass radius of the stellar component, as given in equation (12), for the three limits in the bottom panel.

where $M_{\rm h}(r) = M_{\rm T}(r) - M_*(r)$. In Fig. 1 (top panel) the mass ratios corresponding to the three limits in the bottom panel are shown. The values are smaller than unity for all values of γ, except for the $\gamma = 2$ case.

Another observationally relevant quantity is the projected mass ratio of dark-to-visible, for example within the effective radius $R_{\rm e}$ of the stellar distribution. This is given by

$$\frac{2M_{\rm Ph}(R_{\rm e})}{M_*} \geq \pi(3-\gamma)\mathcal{R}_{\rm m}(\gamma)\eta_{\rm e} - 1, \quad \eta_{\rm e} \equiv R_{\rm e}/r_*, \tag{13}$$

where for example $\eta_{\rm e} \simeq 2.9036$ for $\gamma = 0$ (Dehnen 1993), $\eta_{\rm e} \simeq 2.3585$ for $\gamma = 1/2$, $\eta_{\rm e} \simeq 1.8153$ for $\gamma = 1$ (Hernquist 1990) and $\eta_{\rm e} \simeq 0.7447$ for $\gamma = 2$ (Carollo et al. 1995; note that in Jaffe 1983 the slightly erroneous coefficient 0.763 is reported). These values translate into mass ratios of $\simeq$0.71, 0.70, 0.69 and 1.34 when considering the minimum value of $\mathcal{R}_{\rm m}(\gamma)$ for halo positivity, for $\gamma = 0$, 1/2, 1 and 2, respectively.

3 THE PHASE-SPACE DISTRIBUTION FUNCTION

Before solving the Jeans equations, it is useful to discuss some basic property of the phase-space DF of the presented models, in order to exclude physically inconsistent combinations of parameters (i.e. choices that would correspond to a somewhere negative DF). Fortunately, as discussed extensively in Ciotti & Pellegrini (1992, hereafter CP92), C96 and C99, it is possible to obtain lower bounds for the OM anisotropy radius as a function of the density slope and the total mass profile, without actually recovering the DF, which is in general impossible in terms of elementary functions. More specifically, in CP92 a simple theorem was proved regarding the necessary and sufficient limitations on $r_{\rm a}$ in multicomponent OM models, while more recently An & Evans (2006) proved the so-called 'cusp slope-central anisotropy' theorem (see also equation 28 in de Bruijne et al. 1996); the link between the two results is briefly addressed in Ciotti & Morganti (2008). Before using the CP92 test some preliminary work is however in order, because at variance with the common case of finite total mass, the total potential

$$\phi_{\rm T} = v_{\rm c}^2 \ln s \tag{14}$$

is now quite peculiar, being logarithmic. This means that in principle orbits of any energy can be present, and the standard OM prescription must be reformulated to take into account the divergent behaviour of the potential both at $r = 0$ and ∞. Thus, a DF with the functional dependence

$$f = f(Q), \quad Q \equiv E + \frac{J^2}{2r_{\rm a}^2}, \tag{15}$$

is assumed, where $E = \phi_{\rm T} + v^2/2$ and J are the energy and angular momentum modulus of each star (per unit mass), respectively. Note that, at variance with the usual OM parametrization, no cut on f for negative Q is present. By integration over the velocity space it is easy to show that for a given density component (stars or halo) in the total potential $\phi_{\rm T}$, the density is related to its DF by

$$\rho = \frac{4\pi}{1 + r^2/r_{\rm a}^2} \int_{\phi_{\rm T}}^{\infty} f(Q)\sqrt{2(Q-\phi_{\rm T})}\,{\rm d}Q; \tag{16}$$

in principle, $r_{\rm a}$ can be different for stars and dark matter. The analogy with the standard OM relation is apparent (e.g. see Binney & Tremaine 2008). Following a similar treatment, it can also be shown that the radial ($\sigma_{\rm r}$) and tangential ($\sigma_{\rm t}$) components of the velocity dispersion tensor are related as in the standard OM case, i.e.

$$\beta(r) \equiv 1 - \frac{\sigma_{\rm t}^2(r)}{2\sigma_{\rm r}^2(r)} = \frac{r^2}{r^2 + r_{\rm a}^2}, \tag{17}$$

so that the fully isotropic case is obtained for $r_{\rm a} \to \infty$, while for $r_{\rm a} = 0$ the galaxy is supported by pure radial anisotropy. For finite values of $r_{\rm a}$, the velocity dispersion tensor becomes isotropic for $r \to 0$ (in practice for $r < r_{\rm a}$), and fully radially anisotropic for $r \to \infty$ (in practice for $r > r_{\rm a}$). Introducing the augmented density

$$\varrho(r) \equiv \rho(r)\left(1 + \frac{r^2}{r_{\rm a}^2}\right), \tag{18}$$

equation (16) can be Abel inverted, obtaining

$$\begin{aligned} f(Q) &= \frac{1}{\sqrt{8}\pi^2}\frac{\rm d}{{\rm d}Q}\int_Q^{\infty}\frac{{\rm d}\varrho}{{\rm d}\phi_{\rm T}}\frac{{\rm d}\phi_{\rm T}}{\sqrt{\phi_{\rm T}-Q}} \\ &= \frac{1}{\sqrt{8}\pi^2}\int_Q^{\infty}\frac{{\rm d}^2\varrho}{{\rm d}\phi_{\rm T}^2}\frac{{\rm d}\phi_{\rm T}}{\sqrt{\phi_{\rm T}-Q}}, \end{aligned} \tag{19}$$

where it is intended that ϱ is expressed in terms of $\phi_{\rm T}$, and the second identity follows from integration by parts when considering the untruncated nature of the studied density distributions.

Moreover, for the present class of models it can be also proved that the velocity profile (VP; e.g. Carollo et al. 1995) can be written as

$$\Sigma_* {\rm VP} = 4\pi\int_R^{\infty}\frac{g(r,\,R)r\,{\rm d}r}{\sqrt{r^2-R^2}}\int_{Q_{\rm m}}^{\infty} f(Q)\,{\rm d}Q, \tag{20}$$

© 2009 The Authors. Journal compilation © 2009 RAS, MNRAS **393,** 491–500

with

$$g(r,R)=\frac{r_{\rm a}^2}{\sqrt{r^2+r_{\rm a}^2}\sqrt{r^2+r_{\rm a}^2-R^2}} \tag{21}$$

and

$$Q_{\rm m}=\phi_{\rm T}+\frac{r^2+r_{\rm a}^2}{r^2+r_{\rm a}^2-R^2}\frac{v_{||}^2}{2}, \tag{22}$$

where $v_{||}$ is the velocity along the line of sight direction. The inner integral in equation (20) can be simplified by using the first identity in equation (19).

3.1 Necessary and sufficient conditions for consistency

Repeating the same treatment of CP92, after differentiation of equation (16) with respect to $\phi_{\rm T}$, it follows that a necessary condition (NC) for the positivity of the DF is that

$$\frac{{\rm d}\varrho(r)}{{\rm d}r}\leq 0 \quad [{\rm NC}]. \tag{23}$$

This NC for the DF positivity is independent of the radial dependence of the other density components of the system.

The CP92 weak sufficient condition (WSC) for consistency is recovered by requiring that the second derivative inside the integral in equation (19) be positive. In analogy with equation (23), this condition can be expressed as a function of radius as

$$\frac{\rm d}{{\rm d}r}\left[\frac{{\rm d}\varrho(r)}{{\rm d}r}\frac{r^2}{M_{\rm T}(r)}\right]\geq 0 \quad [{\rm WSC}], \tag{24}$$

where the total mass is given by equation (7).

3.1.1 Isotropic halo consistency

The first application of equations (23) and (24) concerns the consistency of the halo density distribution $\rho_{\rm h}$. For simplicity we restrict to the isotropic case, and then equation (23) shows the equivalence of the request of monotonicity of $\rho_{\rm h}$ discussed in Section 2.2 with the NC for a phase-space consistent halo. The WSC for a fully isotropic halo can be discussed analytically as described in Appendix A, and the resulting limit is represented by the dashed line in Fig. 1 (bottom panel); note how the three conditions of halo positivity, monotonicity and consistency produce very similar curves, that coincide for $\gamma=2$.

Of course, the restriction of the study to an isotropic halo is quite arbitrary, as the virialized end states of N-body collapses are characterized by some amount of orbital anisotropy (e.g. van Albada 1982; Nipoti, Londrillo & Ciotti 2006). However, the present investigation is mainly focused on the properties of the visible component, and therefore we adopt the simplest dynamical structure for the halo.

3.1.2 Anisotropic stellar consistency

In general, when dealing with OM anisotropic systems, the investigation of the NC and WSC (equations 23–24), and the study of the DF positivity (equation 19) lead to inequalities of the kind

$$F+\frac{G}{s_{\rm a}^2}\geq 0 \tag{25}$$

that must hold over all the domain of interest, which we indicate with $\mathcal{C}$. In practice, the functions F and G are radial functions (in the case of the NC and WSC) or functions of the phase-space variable Q (in the case of the DF), depending on the specific context. Following C99, here we recall that according to equation (25) all OM models can be divided in two main families. In the first case, the function F is nowhere negative over $\mathcal{C}$ (this could be the case of a system with a positive isotropic DF). Then, the lower bound to $s_{\rm a}$ is given by

$$s_{\rm a}^-=\sqrt{\max\left[0,\sup_{\mathcal{C}}\left(-\frac{G}{F}\right)\right]}, \tag{26}$$

and the condition (25) is satisfied provided $s_{\rm a}\geq s_{\rm a}^-$; in particular, if G is also positive over $\mathcal{C}$ then the system can be supported by radial orbits only. However, it may happen that F is positive only over some proper subset $\mathcal{C}_+$ of $\mathcal{C}$, and negative (or zero) over $\mathcal{C}_-$. It trivially follows that in this second class of models if G is negative over some subset[1] of $\mathcal{C}_-$, then the condition (25) cannot be satisfied for any value of $s_{\rm a}$. On the contrary, it may happen that G is everywhere positive on $\mathcal{C}_-$: in this case one must consider not only the lower limit $s_{\rm a}^-$ over $\mathcal{C}_+$, but also the upper bound

$$s_{\rm a}^+=\sqrt{\inf_{\mathcal{C}_-}\left(-\frac{G}{F}\right)}, \tag{27}$$

so that $s_{\rm a}^-<s_{\rm a}^+$ over $\mathcal{C}_-$ for consistency. Summarizing, if $F\geq 0$ over all its domain (i.e. $\mathcal{C}_+=\mathcal{C}$), then $s_{\rm a}\geq s_{\rm a}^-$ satisfies inequality (25). If $F\leq 0$ over some set $\mathcal{C}_-$ but $G\geq 0$ there, then the inequality $s_{\rm a}^-\leq s_{\rm a}\leq s_{\rm a}^+$ must be verified. Finally, if over $\mathcal{C}_-s_{\rm a}^+<s_{\rm a}^-$ or $G<0$ somewhere, then inequality (25) cannot be satisfied and, in case of a DF analysis, the model must be rejected as inconsistent.

For example, in the case of γ models the $s_{\rm a}^-(\gamma)$ limit from the NC has been calculated analytically in C99, and the critical value of the anisotropy radius expressed in units of r_* are $\simeq$0.354, $\simeq$0.128 and 0 for $\gamma=0$, 1 and 2, respectively. In other words, smaller values of $s_{\rm a}$ correspond to physically inconsistent models (even though the solution of the associated Jeans equations is positive – see the following section). The anisotropy limit over the whole range of γ here considered is represented with the dotted line in Fig. 2; note how centrally flatter models are associated with larger values of the critical anisotropy radius.

We now discuss the case of the WSC for the stellar component of our models. As shown in Appendix A, simple algebra reveals that the function F in equation (25) is positive everywhere for $\gamma>4/17$, and from equation (A5) the maximum of the function $-G/F$ can be determined by solving an equation of degree four. The resulting value of $s_{\rm a}^-(\gamma)$ is shown with the solid line in Fig. 2. For $0\leq\gamma\leq 4/17$ the function F has two positive roots, delimiting the interval $\mathcal{C}_-$ on which $F<0$. The function G is positive on $\mathcal{C}_-$, so that we can determine the two values $s_{\rm a}^+$ (on $\mathcal{C}_-$) and $s_{\rm a}^-$ (on $\mathcal{C}_+$); however, it turns out that $s_{\rm a}^+<s_{\rm a}^-$ for $0\leq\gamma\leq 4/17$, so that the WSC is not satisfied, and for this reason the solid line interrupts in Fig. 2. Of course, being just a sufficient condition, this result does not exclude that consistent models exist for $\gamma<4/17$, but this is not assured as it is for the models with $\gamma>4/17$. For reference, in Fig. 2 the dashed line represents the WSC for one-component γ models as derived in C99. In particular, note how for models with $\gamma\gtrsim 1$, the presence of the halo appears to increase the model ability to sustain radial orbital anisotropy, while flatter models in presence of the halo are less able to sustain anisotropy.

[1] In C99 and Ciotti (2000) it is erroneously stated that the model is inconsistent if $G<0$ everywhere on $\mathcal{C}_-$. All the results presented therein are however correct.

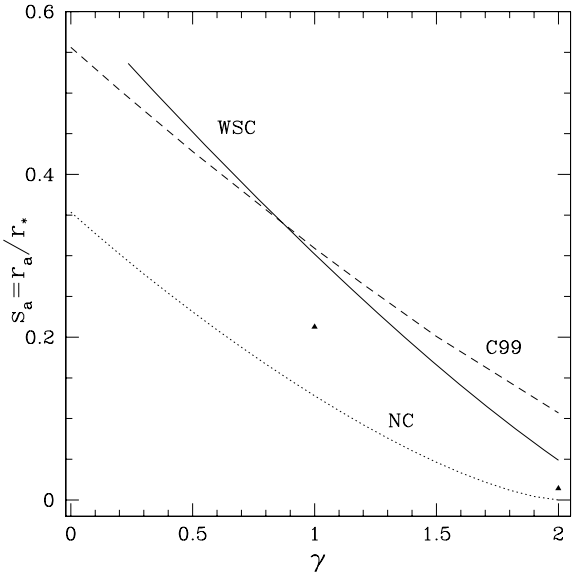

Figure 2. The NC limit for consistency of γ models is shown with the dotted line: all values of the anisotropy radius below the line correspond to inconsistent models (C99). Solid line: the WSC for the present models, i.e. the locus above which the models are certainly consistent. The line begins at $\gamma = 4/17$, as the WSC is not satisfied for centrally flatter models. Dashed line: the WSC for one-component γ models as determined in C99. The triangles are the true anisotropy limits for the $\gamma = 1$ and $\gamma = 2$ models with halo obtained from their DF (Section 3.2).

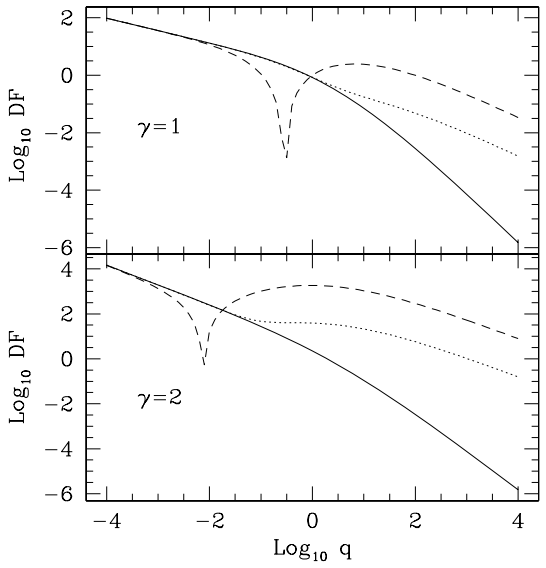

Figure 3. The phase-space DF (normalized to $A_*/{v_c}^3\sqrt{8}\pi^2$) of the stellar component of $\gamma = 1$ (top) and $\gamma = 2$ (bottom) models embedded in a dark matter halo so that the total density profile is proportional to r^{-2}. Solid lines refer to the case of a fully isotropic stellar component, dotted lines to intermediate values of the (normalized) anisotropy radius s_a (1 for $\gamma = 1$ and 0.1 for $\gamma = 2$) and finally the dashed lines to a value of s_a very near to the critical value for consistency.

3.2 Explicit phase-space DF

For generic γ, equation (19) can be rewritten as

$$f(q) = \frac{A_*}{\sqrt{8}\pi^2 v_c^3}\frac{\mathrm{d}}{\mathrm{d}q}\int_q^\infty \frac{\mathrm{d}\tilde{\varrho}}{\mathrm{d}\Psi}\frac{\mathrm{d}\Psi}{\sqrt{\Psi - q}} = \frac{A_*}{\sqrt{8}\pi^2 v_c^3}\left[U(q) + \frac{V(q)}{s_a^2}\right], \quad (28)$$

where $\Psi \equiv \phi_T/v_c^2$ and $q \equiv Q/v_c^2$. The function $\tilde{\varrho}$ is the augmented density in equation (18) normalized to A_*, expressed in terms of the total potential. This is accomplished by elimination of the radius from the dimensionless identity $s = \exp(\Psi)$ obtained from equation (14). Not surprisingly, for generic γ the functions U and v cannot be expressed in terms of known functions; however, in Appendix B it is shown that for $\gamma = 0$, 1 and 2 the functions U and v can be expressed as simple linear combinations of exponentials and polylogarithms. Numerical inspection of the DFs shows that for $\gamma = 1$ and 2 the isotropic component U is positive for all values of q, and the lower bound on the anisotropy limit are $s_a^- = 0.212\,675$ (for $\gamma = 1$) and $s_a^- = 0.0141$ (for $\gamma = 2$). These two limits are represented as solid triangles in Fig. 2. As expected, their position is found between the NC and the WSC loci. Instead, in the $\gamma = 0$ case the function U is negative and the function v is positive for $q \lesssim -2.4$, however, $s_a^- > s_a^+$, and the model is inconsistent. Note that the OM anisotropy limit for γ models without dark halo, derived in C99 from their DF, is $s_a^-(0) \simeq 0.445$, $s_a^-(1) \simeq 0.202$ and $s_a(2) = 0$, so we conclude that the presence of the DM halo slightly reduces the ability of the stellar density distribution to sustain radial anisotropy.

In Fig. 3 the DFs of $\gamma = 1$ and $\gamma = 2$ models are presented, in the isotropic (solid), mildly anisotropic (dotted) and maximally anisotropic (dashed) cases. The dashed curves are very similar to the analogous curves in Ciotti & Lanzoni (1997, fig. 2), and C99 (figs 2 and 3), revealing the common qualitative behaviour of OM anisotropic DFs near the consistency limit, i.e. the fact that the inconsistency manifests itself in general at intermediate energies (see also Ciotti & Morganti 2008 for a discussion).

4 JEANS EQUATIONS WITH OM ANISOTROPY

4.1 Spatial velocity dispersion

The solution of the spherical Jeans equations with general (radial or tangential) anisotropy has been given by Binney & Mamon (1982) and for OM systems is given by

$$\rho_*\sigma_r^2 = \frac{G}{r^2 + r_a^2}\int_r^\infty \rho_*(r)M_T(r)\left(1 + \frac{r_a^2}{r^2}\right)\mathrm{d}r = A_* v_c^2 \frac{A(s) + s_a^2 I(s)}{s^2 + s_a^2}, \quad (29)$$

where $s_a = r_a/r_*$. For the present models the explicit expression of the functions A and I are given in Appendix C for generic γ, however, the resulting formulae are not particularly illuminating, as is common for this kind of models. None the less, it is of some interest that in the $\gamma = 0$ case the velocity dispersion does not present 'unreasonable' behaviour, even though we know that the model is physically inconsistent. Instead, the asymptotic analysis of σ_r^2 at large radii and near the centre provides helpful information that will be used when discussing the projected velocity dispersion profile of the models.

In the radial region $r \gg r_*$, both A and I can be easily evaluated, because the stellar density profile is asymptotic to the r^{-4} profile independently of γ. In any case σ_r^2 tends to a constant: this is not surprising, as an elementary integration shows that the velocity dispersion profile of power-law densities in a total density profile r^{-2} tends to a constant. In fact, an explicit calculation (or the expansion

© 2009 The Authors. Journal compilation © 2009 RAS, MNRAS **393,** 491–500

of equations C1–C3) shows that for $s \to \infty$,

$$\sigma_r^2 \sim v_c^2 \frac{2s^2 + s_a^2}{4\left(s^2 + s_a^2\right)}. \tag{30}$$

Therefore, in the fully isotropic case ($s_a \to \infty$) the radial velocity dispersion at large radii is half of the model circular velocity. If some radial anisotropy is present, then at $r \gg r_a$ the orbital distribution becomes fully radially anisotropic, and accordingly the (square) intrinsic radial velocity dispersion increases by a factor of 2 when compared to the isotropic case.

The situation is more delicate for $r \to 0$. In fact, from asymptotic expansion of the integral in equation (29) it follows that the central behaviour of σ_r is coincident with that of the isotropic case, and the product $\rho_* \, {\sigma_r}^2$ diverges for $r \to 0$ independently of the value of r_a and γ. In addition, for $r_a > 0$ and $\gamma > 0$, the product $\rho_* \, \sigma_r^2$ diverges as ρ_*, so that σ_r^2 converges to a finite value except for the $\gamma = 0$ models:

$$\sigma_r^2 \sim v_c^2 \begin{cases} -\log s, & (\gamma = 0), \\ \dfrac{1}{\gamma}, & (0 < \gamma \leq 2). \end{cases} \tag{31}$$

This is relevant from the modelistic point of view, as it is well known that self-gravitating isotropic γ models present a depression of their velocity dispersion near the centre with $\sigma_r(0) = 0$ (except for the $\gamma = 0$ and $\gamma = 2$ models, see Bertin, Ciotti & Del Principe 2002 for a general discussion of this phenomenon; see also Binney & Ossipkov 2001).

Before discussing the projected velocity dispersion, it can be of interest in applications to have the analytical expression of the total kinetic energy of the stellar component. As is well known, from the virial theorem this quantity is independent of the specific orbital anisotropy considered, and can be obtained without using the explicit solution of the Jeans equations. In fact $2K_* \equiv \int \rho_* \mathrm{Tr}(\sigma^2)\, \mathrm{d}^3\boldsymbol{x} = \int \langle \boldsymbol{x}, \nabla\phi_T \rangle \rho_* \, \mathrm{d}^3\boldsymbol{x} = 4\pi G \mathcal{R} M_* A_* r_*^2$, where the last identity holds for any system of finite total mass M_* in the gravitational field of the density distribution (6) (see also Kochanek 1994), and in the present case

$$K_* = \frac{G M_*^2}{r_*} \frac{(3-\gamma)\mathcal{R}}{2}. \tag{32}$$

Thus, if one defines the one-dimensional stellar virial velocity dispersion as $3\, M_* \, \sigma_V^2/2 = K_*$, it follows from the equation above that

$$\sigma_V^2 = \frac{G M_*}{r_*} \frac{(3-\gamma)\mathcal{R}}{3} = \frac{v_c^2}{3}, \tag{33}$$

independently of the value of γ.

4.2 Stability

Equations (29) and (32) can be used to obtain indications about the minimum admissible value of s_a as a function of γ to prevent the onset of radial orbit instability. A complete stability analysis is beyond the task of this work, requiring *N*-body simulations or normal mode analysis, but some interesting conclusions can be equally derived from the work of Fridman & Polyachenko (1984). These authors argued that a quantitative indication on the maximum amount of radial anisotropy sustainable by a specific density profile is given by the stability parameter $\xi \equiv 2K_{r*}/K_{t*}$, where K_{r*} and $K_{t*} = K_* - K_{r*}$ are the radial and tangential component of the kinetic energy tensor, respectively. From its definition $\xi \to 1$ for $s_a \to \infty$ (globally isotropic models), while $\xi \to \infty$ for $s_a \to 0$ (fully radially anisotropic models), and for one-component systems stability is associated with the empirical requirement that $\xi < \xi_c = 1.7 \pm 0.25$; the exact value of ξ_c is model dependent (see e.g. Merritt & Aguilar 1985; Bertin & Stiavelli 1989; Saha 1991, 1992; Bertin et al. 1994a; Meza & Zamorano 1997; Nipoti, Londrillo & Ciotti 2002). Here we are considering two-component systems, however, *N*-body simulations have shown that the presence of a halo does not change very much the situation with respect to the one-component systems (e.g. see Stiavelli & Sparke 1991; Nipoti et al. 2002). Therefore, in the following discussion we assume as a fiducial maximum value for stability $\xi_c = 1.7$.

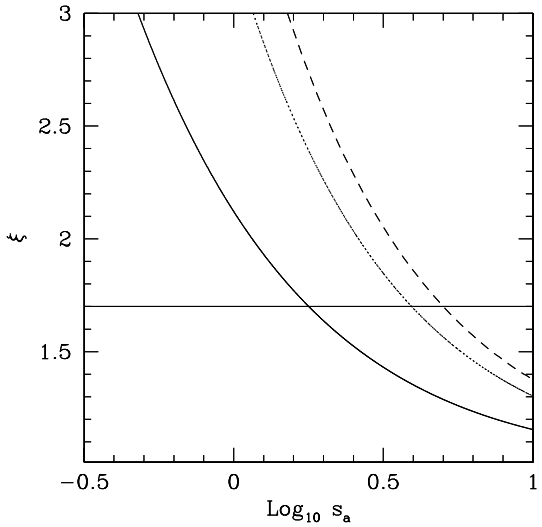

Figure 4. The stability indicator ξ as a function of the normalized anisotropy radius $s_a = r_a/r_*$, for models with $\gamma = 1/2$, 1, 2 (dashed, dotted and solid lines, respectively). The horizontal line marks the fiducial stability limits $\xi_c = 1.7$.

The parameter ξ for the present models is independent of $\mathcal{R}$, and it cannot be expressed by using elementary functions, so that we explore its value numerically. In Fig. 4 we plot ξ as a function of s_a for $\gamma = 1/2$, 1 and 2, and the asymptotic flattening to unity for increasing isotropy is evident. It is apparent that the stability criterion requires minimum anisotropy radii appreciably larger than those obtained from the consistency analysis (see Section 3.2). In addition, stable stellar distributions with shallower central density profile require more and more isotropic velocity dispersion, confirming the trend already found for one- and two-component γ models (e.g. Carollo et al. 1995; C96; C99). So, it is likely that the more radially anisotropic models with positive DF are prone to radial orbit instability.

4.3 Projected velocity dispersion

The projected velocity dispersion associated with a general anisotropy function $\beta(r)$ (see equation 17) is given by

$$\Sigma_*(R)\sigma_p^2(R) = 2\int_R^\infty \left[1 - \beta(r)\frac{R^2}{r^2}\right] \frac{\rho_*(r)\sigma_r^2(r)\, r}{\sqrt{r^2 - R^2}}\, \mathrm{d}r. \tag{34}$$

Unfortunately the projection integral above cannot be evaluated analytically for generic γ in terms of elementary functions. However, as for the projected stellar density, interesting information can be obtained in two relevant radial regions, i.e. outside the core radius and near the centre. In practice, the external regions are defined as the radial interval where the stellar density profile can be approximated as a pure power law of slope -4. In this region the projection

integral can be evaluated for generic values of s_a and the asymptotic result is

$$\sigma_p^2(R) \sim v_c^2 \frac{\left(s_a^2+\eta^2\right)^{5/2} - \eta^3\left(2s_a^2+\eta^2\right)}{4s_a^2\left(s_a^2+\eta^2\right)^{3/2}}, \quad (35)$$

where $\eta \equiv R/r_*$. In the fully isotropic case the dimensionless ratio $\sigma_p(R)/v_c$ tends to 1/2, so that the projected velocity dispersion coincides with the (constant) isotropic velocity dispersion (as expected), while in the completely radially anisotropic case (or for $\eta \gg s_a$) the ratio converges to $1/\sqrt{8}$.

The case of the central regions is more complicated. In fact, integral (34) for $R \to 0$ converges when $0 \le \gamma < 1$, and diverges for $1 \le \gamma \le 2$, as can be easily proved by using equations (C5) and (C6). In the divergent case both the projection integral and the projected surface density Σ_* are asymptotically dominated by their integrands for $r \sim 0$ (as is intuitive, the cusp dominates and the contribution of foreground stars and background stars is negligible), and $\sigma_p(R)$ can be properly defined as the limit value of their ratio for $R \to 0$. A simple calculation shows that

$$\sigma_p(0) = \sigma_r(0) = \frac{v_c}{\sqrt{\gamma}}, \quad 1 \le \gamma \le 2. \quad (36)$$

In other words, for the models with the centrally divergent surface (stellar) density, the projected central velocity dispersion coincides with the central radial component of the isotropic velocity dispersion. Thus it does not depend on the model anisotropy radius, at variance with the projected velocity dispersion in the external galactic regions.

In the convergent case $0 \le \gamma < 1$ the central value of the projection integral depends on the whole profile of the integrand, therefore, the projected central velocity dispersion depends also on s_a. For generic γ and s_a, the quantity $\sigma_p(0)$ is expressible in terms of hypergeometric ${}_2F_1$ functions. However, a simple form of the projection integral evaluated at $R = 0$, useful in numerical integrations, can be obtained by inverting the order of integration in equation (34):

$$\Sigma_*(0)\sigma_p^2(0) = 2\int_0^\infty \rho_*(r)\sigma_r^2(r)\,\mathrm{d}r = \frac{8\pi G\mathcal{R}A_*^2 r_*^3}{s_a} \times \int_0^\infty \frac{s^{1-\gamma}}{(1+s)^{4-\gamma}}\left(1+\frac{s_a^2}{s^2}\right)\arctan\frac{s}{s_a}\,\mathrm{d}s. \quad (37)$$

In the fully isotropic case ($s_a \to \infty$) the projection integral can be evaluated analytically and the result is

$$\sigma_p(0) = v_c, \quad 0 \le \gamma < 1, \quad (38)$$

which is independent of γ. This is not surprising, as it is easy to show, by inverting order of integration, that for any density profile with finite central projected density, isotropic orbital distribution, in the total gravitational field produced by density distribution (6), identity (38) holds.

Equations (35), (36) and (38) open the interesting possibility to consider the ratio of the outer to the central projected velocity dispersion, a quantity that can be expressed in a very simple way. In particular, the ratio depends on the shape of the stellar density slope γ, on the outer observational point R and finally on s_a. Thus, at least in principle, for galaxies well described by a γ model immersed in a total density profile $\propto r^{-2}$, it could be possible to determine s_a from observations, assuming OM anisotropy. In Fig. 5 the ratio is plotted as a function of the anisotropy radius for the representative values of the density slope 2, 1 and 1/2 (in this latter case the WSC limit for consistency is $s_a \gtrsim 0.45$). All the expected trends are apparent, in particular the decrease of the ratio $\sigma_p(R)/\sigma_p(0)$ for decreasing s_a. This is due, for $1 \le \gamma \le 2$, to the decrease of $\sigma_p(R)$ in the external regions of radially anisotropic models. In the $\gamma = 1/2$ case, reported as an example of models with central slope in the range $0 \le \gamma < 1$, the larger decrease is due to the additional effect of the increase of $\sigma_p(0)$ for decreasing s_a. Overall, the kinematical ratio $\sigma_p(R)/\sigma_p(0)$ for mildly strongly anisotropic models (i.e. $s_a \lesssim 1$) is ∼15–20 per cent lower than in the corresponding isotropic cases.

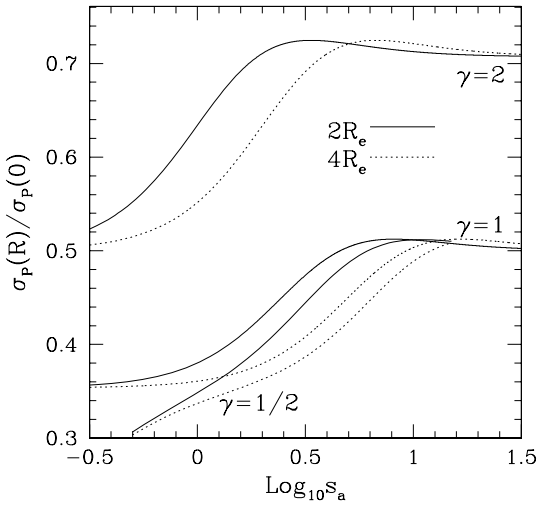

Figure 5. The ratio $\sigma_p(R)/\sigma_p(0)$ as a function of the normalized anisotropy radius $s_a = r_a/r_*$, for models with $\gamma = 1/2$, 1 and 2. Solid lines refer to $R = 2R_e$, dotted lines to $R = 4R_e$.

4.4 Some additional considerations

For sake of completeness, we summarize some additional results on velocity dispersion. For example, the central velocity dispersion of γ models in the presence of a black hole can be found in the literature. Here we just recall that the velocity dispersion diverges for $r \to 0$ as $r^{-1/2}$ (e.g. see C96, Baes & Dejonghe 2004; Baes et al. 2005; for the case of oblate γ models, or two-component oblate power-law models with central black hole see also Ciotti & Bertin 2005; Riciputi et al. 2005). It follows that in the present context a central black hole would produce an identical kinematical signature, as sufficiently near the centre the total mass is fully dominated by the black hole.

As a second case, we consider the spatial and projected velocity dispersion of a two-component galaxy model made by the superposition of a stellar component described by a γ model (where for simplicity we restrict to the interval $1 \le \gamma \le 2$), and a dark halo component described by a Jaffe model ($\gamma = 2$). The interest of these models is due to the fact that in the inner regions they behave as the models subject of this work, but in the external regions a Keplerian decline is present, due to the halo finite total mass. From equation (1), the Jaffe profile of total mass $M_h = \mathcal{R}M_*$ and scalelength $r_h = \beta r_*$ can be written as

$$\rho_h(r) = \frac{A_*\mathcal{R}\beta}{(3-\gamma)\,s^2(\beta+s)^2}. \quad (39)$$

The Jeans equations for this class of models cannot be solved explicitly in terms of elementary functions for generic γ, even though special explicit cases can be easily found (e.g. see Ciotti et al. 1996). For this reason we just evaluate the asymptotic leading term of the velocity dispersion for $s \to \infty$, obtaining

$$\sigma_r{}^2 \sim \frac{GM_*(1+\mathcal{R})}{r_*}\frac{5s^2+3s_a^2}{15s\left(s^2+s_a^2\right)}, \quad (40)$$

© 2009 The Authors. Journal compilation © 2009 RAS, MNRAS **393,** 491–500

and its projection through equation (34), giving

$$\sigma_{\rm p}{}^2(R) \sim \frac{GM_*}{r_*}\frac{4(1+\mathcal{R})}{15\pi\eta}\left[2+\frac{\eta^4}{s_{\rm a}^2\left(s_{\rm a}^2+\eta^2\right)}\right.$$
$$\left.-\frac{\eta^4\left(2s_{\rm a}^2+\eta^2\right)\sinh^{-1}(s_{\rm a}/\eta)}{s_{\rm a}^3\left(s_{\rm a}^2+\eta^2\right)^{3/2}}\right], \qquad (41)$$

where $\eta \equiv R/r_*$. The expression in square bracket converges to 2 in the isotropic case.

The behaviour of the velocity dispersion in the central regions requires some additional discussion. In fact, for $1 \leq \gamma \leq 2$ the central projected velocity dispersion will depend on the central, isotropic spatial velocity dispersion only (for the reasons described in Section 4.2, and excluding the purely radial case). In addition, the self-contribution to the central velocity dispersion of the γ model is zero (except for the $\gamma = 2$ case, e.g. see Bertin et al. 2002). Summarizing, the projected central velocity dispersion of these models is coincident with the isotropic spatial velocity dispersion of γ models in the presence of the Jaffe halo only (with the exception of the $\gamma = 2$ case). Therefore,

$$\sigma_{\rm p}^2(0) = \sigma_{\rm r}^2(0) = \frac{GM_*}{r_*}\begin{cases}\dfrac{\mathcal{R}}{\beta\gamma}, & (1 \leq \gamma < 2),\\ \dfrac{\beta+\mathcal{R}}{2\beta}, & (\gamma = 2).\end{cases} \qquad (42)$$

4.5 Velocity profile

Not surprisingly, the VP cannot be expressed in terms of elementary functions, however, acceptably simple formulae can be obtained at large radii and in the central galactic regions. The starting point is to consider the normalization of equation (20), given by

$$\Sigma_* {\rm VP} = -\frac{\sqrt{2}}{\pi}\frac{A_* r_*}{v_{\rm c}}\int_\eta^\infty \frac{g(s,\eta)sG(q_{\rm m})\,{\rm d}s}{\sqrt{s^2-\eta^2}}, \qquad (43)$$

where $q_{\rm m} \equiv Q_{\rm m}/v_{\rm c}^2$, and

$$G(q_{\rm m}) = \int_{q_{\rm m}}^\infty \frac{{\rm d}\tilde{\varrho}}{{\rm d}\Psi}\frac{{\rm d}\Psi}{\sqrt{\Psi - q_{\rm m}}}. \qquad (44)$$

At the very centre of the stellar system, where the stellar density profile is proportional to $s^{-\gamma}$, it is not difficult to show that for $1 \leq \gamma \leq 2$,

$${\rm VP} \sim \sqrt{\frac{\gamma}{2\pi v_{\rm c}^2}}\,{\rm e}^{-\gamma v_{||}^2/2v_{\rm c}^2} \qquad (45)$$

independently of the (positive) value of the anisotropy radius. Instead, for $0 \leq \gamma < 1$, as for the projected velocity dispersion a numerical integration is required.

In the external galactic regions, where the stellar density profile can be approximated as s^{-4} power law, the VP can be written as a quite simple integral, depending on the dimensionless ratios $v_{||}/v_{\rm c}$ and $\eta/s_{\rm a}$, that can be evaluated numerically. Here we just report the formula for the isotropic case, where

$${\rm VP} \sim \sqrt{\frac{2}{\pi v_{\rm c}^2}}\,{\rm e}^{-2v_{||}^2/v_{\rm c}^2}. \qquad (46)$$

In both the reported formulae, the Gaussian signature is apparent.

5 CONCLUSIONS

In this paper a family of spherical, two-component galaxy models with a stellar density profile described by a γ model and a total (stars plus dark matter) density profile $\propto r^{-2}$ at all radii has been investigated, under the assumption that the internal dynamics of the stellar component is described by OM anisotropy. The models are fully determined when the inner density slope γ and the anisotropy radius $r_{\rm a}$ of the stellar component are assigned, together with a density scale for the total density profile. The dark matter halo remains defined as the difference between the total and stellar density profiles. The main results can be summarized as follows.

(i) After having provided the most common structural quantities of the models that are of interest for observations, limitations on the total density scale as a function of γ are analytically determined by requiring the positivity and monotonicity of the dark matter halo distribution. In particular, the request of positivity limits the range of acceptable stellar density slopes to $0 \leq \gamma \leq 2$. Models corresponding to the minimum total density scale (for given γ) are called minimum halo models. The central density profile of the dark matter halo diverges as r^{-2} in general, but in the minimum halo $\gamma = 2$ model (in which the positivity and monotonicity limits coincide), the central dark matter profile is $\propto r^{-1}$.

(ii) The minimum value of anisotropy radius corresponding to a dynamically consistent stellar component has been derived analytically as a function of γ by using the necessary and sufficient conditions of CP92. As expected, an increase of γ results in a decrease of the minimum value of the anisotropy radius $r_{\rm a}$ required by consistency. It is also proved that models with $\gamma > 4/17$ are certainly consistent for sufficiently isotropic velocity dispersion, while for centrally shallower stellar density profiles the sufficient condition for consistency is never satisfied. The necessary and sufficient conditions for the halo consistency are also analytically obtained, and the minimum halo models corresponding to (isotropic) dark matter haloes are derived. In the case $\gamma = 2$, the minimum halo coincides with the minimum halo obtained from the positivity and monotonicity conditions.

(iii) The phase-space DF of the stellar component for $\gamma = 0$, 1, 2 is analytically recovered in terms of polylogarithms and exponentials. It is found that the $\gamma = 0$ model is inconsistent no matter how much anisotropy is considered. Instead, the isotropic $\gamma = 1$, 2 models have a positive DF, and the true critical anisotropy radius for consistency can be determined directly from their DF. A comparison with the analogous study of one-component γ models shows that the presence of the halo slightly reduces the maximum amount of sustainable radial anisotropy. The obtained values of the anisotropy radius are independent of the total density scale $\mathcal{R}$.

(iv) The Jeans equations for the stellar component are solved explicitly for generic values of γ and $r_{\rm a}$ in terms of elementary functions. The asymptotic expansions of $\sigma_{\rm r}$ for $r \to 0$ and $r \to \infty$ are obtained, and it is shown that $\sigma_{\rm r}$ tends to finite (non-zero) values (except for the divergent central velocity dispersion of $\gamma = 0$ model) which are simply related to the model circular velocity. The projected velocity dispersion $\sigma_{\rm p}(0)$ cannot be calculated analytically, in general. However, by asymptotic expansion of the projection integral, exact values at large radii and at the centre are obtained. In particular, it is shown that for $\gamma \geq 1$, and independently of the value of the anisotropy radius, $\sigma_{\rm p}(0)$ coincides with the central velocity dispersion $\sigma_{\rm r}(0)$ in the isotropic case. Instead, for $0 \leq \gamma < 1$, $\sigma_{\rm p}(0)$ depends also on $s_{\rm a}$. In the anisotropic case $\sigma_{\rm p}(0)$ cannot be obtained analytically; however, a very simple form of the projection integral suitable for numerical integrations is given. In the isotropic case the integral can be evaluated analytically, and $\sigma_{\rm p}(0)$, as expected, coincides with the model circular velocity.

(v) Finally, we have shown that the VP of the models can be obtained in a very simple form (Gaussian) near the centre (independently of the value of the anisotropy radius and for $1 \leq \gamma \leq 2$), and at large radii (in the isotropic case).

We conclude by noting that these models, albeit highly idealized, seem to suggest two interesting remarks of observational character. The first is that in real galaxies with a total r^{-2} density profile and sufficiently peaked stellar density (i.e. $\gamma \geq 1$), measures of central velocity dispersion should not be strongly affected by radial anisotropy. Second, for given central stellar density slope γ, measures of the projected velocity dispersion at the centre and in the external regions are able, at least in principle, to determine the value of the anisotropy radius under the assumption of OM anisotropy.

ACKNOWLEDGMENTS

LC wishes to thank Carlo Nipoti and Leon Koopmans for useful comments. We also thank an anonymous referee for useful comments.

REFERENCES

An J. H., Evans W., 2006, ApJ, 642, 752
Baes M., Dejonghe H., 2004, MNRAS, 351, 18
Baes M., Dejonghe H., Buyle P., 2005, A&A, 432, 411
Bertin G., Stiavelli M., 1989, ApJ, 338, 723
Bertin G., Pegoraro F., Rubini F., Vesperini E., 1994a, ApJ, 434, 94
Bertin G. et al., 1994b, A&A, 292, 381
Bertin G., Ciotti L., Del Principe M., 2002, A&A, 386, 149
Binney J., Mamon G., 1982, MNRAS, 200, 361
Binney J., Ossipkov L. P., 2001, in Ossipkov L. P., Nikiforov I. I., eds, Proc. Int. Conf., Stellar Dynamics: From Classic to Modern. Sobolev Astronomical Institute, Saint Petersburg, p. 317
Binney J., Tremaine S., 2008, Galactic Dynamics, 2nd edn. Princeton Univ. Press, Princeton, NJ
Buyle P., Hunter C., Dejonghe H., 2007, MNRAS, 375, 773
Cappellari M. et al., 2007, MNRAS, 379, 418
Carollo C. M., de Zeeuw P. T., van der Marel R. P., 1995, MNRAS, 276, 1131
Ciotti L., 1996, ApJ, 471, 68 (C96)
Ciotti L., 1999, ApJ, 520, 574 (C99)
Ciotti L., 2000, Lecture Notes on Stellar Dynamics. Scuola Normale Superiore, Pisa, Italy
Ciotti L., Bertin G., 2005, A&A, 437, 419
Ciotti L., Lanzoni B., 1997, A&A, 321, 724
Ciotti L., Morganti L., 2008, in press (arXiv:0811.0322G)
Ciotti L., Pellegrini S., 1992, MNRAS, 255, 561 (CP92)
Ciotti L., Lanzoni B., Renzini A., 1996, MNRAS, 282, 1
Czoske O., Barnabe M., Koopmans L. E. V., Treu T., Bolton A. S., 2008, ApJ, 384, 987
de Bruijne J. H. J., van der Marel R. P., de Zeeuw P. T., 1996, MNRAS, 282, 909
Dehnen W., 1993, MNRAS, 265, 250
Dye S., Evans N. W., Belokurow V., Warren S. J., Hewett P., 2008, MNRAS, 388, 384
Erdélyi A., Magnus W., Oberhettinger F., Tricomi F. G., 1953, Higher Transcendental Functions, Vol. 1. McGraw-Hill, New York
Fridman A. M., Polyachenko V. L., 1984, Physics of Gravitating Systems. Springer-Verlag, New York
Gavazzi R., Treu T., Rhodes J. D., Koopmans L. V. E., Bolton A. S., Burles S., Massey R. J., Moustakas L. A., 2007, ApJ, 667, 176
Gerhard O., Kronawitter A., Saglia R. P., Bender R., 2001, AJ, 121, 1936
Hernquist L., 1990, ApJ, 536, 359
Hiotelis N., 1994, A&A, 291, 725
Jaffe W., 1983, MNRAS, 202, 995
Keeton C. R., 2001, ApJ, 561, 46
Kochanek C. S., 1994, ApJ, 436, 56
Koopmans L. V. E., Treu T., Bolton A. S., Burles S., Moustakas L. A., 2006, ApJ, 649, 599
Merritt D., 1985, AJ, 90, 1027
Merritt D., Aguilar L. A., 1985, MNRAS, 217, 787
Meza A., Zamorano N., 1997, AJ, 490, 136
Naab T., Ostriker J. P., 2007, MNRAS, 366, 899
Nipoti C., Londrillo P., Ciotti L., 2002, MNRAS, 332, 901
Nipoti C., Londrillo P., Ciotti L., 2006, MNRAS, 370, 681
Nipoti C., Treu T., Bolton A. C., 2008, MNRAS, 390, 349
Osipkov L. P., 1979, Pis'ma Astron. Zh., 5, 77
Riciputi A., Lanzoni B., Bonoli S., Ciotti L., 2005, A&A, 443, 133
Rix H. W., de Zeeuw P. T., Cretton N., van der Marel R. P., Carollo C. M., 1997, ApJ, 488, 702
Rusin D., Kochanek C. S., 2005, ApJ, 623, 666
Rusin D., Kochanek C. S., Keeton C. R., 2003, ApJ, 595, 29
Saha P., 1991, MNRAS, 148, 494
Saha P., 1992, MNRAS, 254, 132
Stiavelli M., Sparke L. S., 1991, ApJ, 382, 466
Thomas J., Saglia R. P., Bender R., Thomas D., Gebhardt K., Magorrian J., Corsini E. M., Wegner G., 2007, MNRAS, 382, 657
Tremaine S., Richstone D. O., Byun Y., Dressler A., Faber S. H., Grillmair C., Kormendy J., Laver T. R., 1994, AJ, 107, 634
Treu T., Koopmans L. V. E., 2002, ApJ, 575, 87
Treu T., Koopmans L. V. E., 2004, ApJ, 611, 739
van Albada T. S., 1982, MNRAS, 201, 939
van den Bosch R. C. E., van de Ven G., Verolme E. K., Cappellari M., de Zeeuw P. T., 2008, MNRAS, 385, 647

APPENDIX A: NECESSARY AND SUFFICIENT CONDITIONS FOR MODEL CONSISTENCY

The condition for the positivity of the halo density profile $\rho_{\rm h}$ can be easily established from equation (10). In fact, for $0 \leq \gamma \leq 2$, $\mathcal{R}$ must be greater or equal to the maximum of the radial function inside the parentheses, and simple algebra shows that the maximum is attained for

$$s_{\rm m} = \frac{2-\gamma}{2}; \tag{A1}$$

in particular, for the Jaffe model the critical point is reached at the centre. The monotonicity condition is obtained requiring that the radial derivative of $\rho_{\rm h}$ is nowhere positive, and this happens if and only if

$$\mathcal{R} \geq \frac{s^{2-\gamma}(\gamma+4s)}{2(1+s)^{5-\gamma}} \quad \forall s \geq 0. \tag{A2}$$

Thus, $\mathcal{R}$ must be greater than or equal to the maximum of the radial function above, that is reached at

$$s_{\rm m} = \frac{12-7\gamma+\sqrt{(4-\gamma)(36-17\gamma)}}{16}, \tag{A3}$$

and again for $\gamma = 2$ the maximum is reached at the centre. Finally, the application of the WSC to an isotropic halo in order to have phase-space consistency is given by equation (24) with $r_{\rm a} \to \infty$, so that $\varrho = \rho_{\rm h}$. The condition becomes

$$\mathcal{R} \geq \frac{s^{2-\gamma}[16s^2+(9\gamma-4)s+\gamma^2]}{4(1+s)^{6-\gamma}} \quad \forall s \geq 0. \tag{A4}$$

The study of the maximum of the right-hand side (rhs) of equation above leads to a cubic equation. We do not report here the solution $s_{\rm m}(\gamma)$ corresponding to the maximum, as it can be easily obtained, but for reference we just report three special values $s_{\rm m}(0) \simeq 2.2049$, $s_{\rm m}(1) \simeq 1.2079$ and $s_{\rm m}(2) = 0$, corresponding to $\mathcal{R}_{\rm m}(0) \simeq 0.07735$, $\mathcal{R}_{\rm m}(1) \simeq 0.17487$ and $\mathcal{R}_{\rm m}(2) = 1$, respectively.

The application of the WSC to the stellar component reduces instead to the study of

$$16s^2 + (9\gamma - 4)s + \gamma^2 + s^2\frac{4s^2 + (5\gamma - 12)s + (\gamma - 2)^2}{s_a^2} \geq 0, \tag{A5}$$

so that the function F in equation (25) is a quadratic polynomial, and the determination of the sets $\mathcal{C}_+$ and $\mathcal{C}_-$ is straightforward. In particular, $\mathcal{C}_-$ is not empty for $0 \leq \gamma \leq 4/17$, and the function G is positive there.

APPENDIX B: PHASE-SPACE DF FOR THE STELLAR COMPONENT

Here we give the explicit evaluation of the DF for the three integer values $\gamma = 0, 1, 2$. In fact, in these cases one can change the variable integration by defining $t = \sqrt{\Psi - q}$, so that $\mathrm{e}^{\Psi} = \mathrm{e}^{t^2+q}$ and the integration interval is mapped into $(0, \infty)$. Expansion in simple fractions, factorization of e^q outside the integrals and repeated differentiation with respect to e^{-q} under the sign of the integral finally shows that for $\gamma = 0$,

$$U(q) = \frac{\sqrt{\pi}}{6} \times [\mathrm{Li}_{-9/2}(y) - 6\mathrm{Li}_{-7/2}(y) + 11\mathrm{Li}_{-5/2}(y) - 6\mathrm{Li}_{-3/2}(y)], \tag{B1}$$

$$V(q) = \frac{\sqrt{\pi}}{6}[\mathrm{Li}_{-9/2}(y) - \mathrm{Li}_{-5/2}(y)], \tag{B2}$$

where $y \equiv -\mathrm{e}^{-q}$, $\mathrm{Li}_s(z) = z\Phi(z, s, 1)$ is the so-called polylogarithm function, $\Phi(z, s, a)$ is the Lerch function and $\mathrm{dLi}_s(z)/\mathrm{d}z = \mathrm{Li}_{s-1}(z)/z$ (e.g. Erdélyi et al. 1953). A similar treatment for the $\gamma = 1$ case gives

$$U(q) = \frac{\sqrt{\pi}}{2} \times [\mathrm{e}^{-q} + \mathrm{Li}_{-7/2}(y) - 5\mathrm{Li}_{-5/2}(y) + 6\mathrm{Li}_{-3/2}(y)], \tag{B3}$$

$$V(q) = \frac{\sqrt{\pi}}{2}\left[\mathrm{Li}_{-7/2}(y) - \mathrm{Li}_{-5/2}(y)\right], \tag{B4}$$

and finally for $\gamma = 2$

$$U(q) = \sqrt{\pi}\left[2^{3/2}\mathrm{e}^{-2q} - 2\mathrm{e}^{-q} + \mathrm{Li}_{-5/2}(y) - 3\mathrm{Li}_{-3/2}(y)\right], \tag{B5}$$

$$V(q) = \sqrt{\pi}\left[\mathrm{Li}_{-5/2}(y) - \mathrm{Li}_{-3/2}(y)\right]. \tag{B6}$$

APPENDIX C: VELOCITY DISPERSIONS

The isotropic function I in equation (29) for $\gamma \neq 0, 1, 2$ is given by

$$I = \frac{6s^3 + 6(3-\gamma)s^2 + 3(3-\gamma)(2-\gamma)s + (3-\gamma)(2-\gamma)(1-\gamma)}{s^\gamma(1+s)^{3-\gamma}(3-\gamma)(2-\gamma)(1-\gamma)\gamma} - \frac{6}{(3-\gamma)(2-\gamma)(1-\gamma)\gamma}, \tag{C1}$$

while

$$I = \begin{cases} \log\dfrac{1+s}{s} - \dfrac{11 + 15s + 6s^2}{6(1+s)^3}, & \gamma = 0, \\ \dfrac{1}{s} + \dfrac{5+4s}{2(1+s)^2} - 3\log\dfrac{1+s}{s}, & \gamma = 1, \\ 3\log\dfrac{1+s}{s} + \dfrac{1-3s-6s^2}{2s^2(1+s)}, & \gamma = 2. \end{cases} \tag{C2}$$

The function A is given by

$$A = \begin{cases} \dfrac{1}{(3-\gamma)(2-\gamma)} - \dfrac{(3-\gamma+s)s^{2-\gamma}}{(3-\gamma)(2-\gamma)(1+s)^{3-\gamma}}, \\ \log\dfrac{1+s}{s} - \dfrac{1}{1+s}, \qquad \gamma = 2. \end{cases} \tag{C3}$$

For $s \to \infty$ and $0 \leq \gamma \leq 2$,

$$I \sim \frac{1}{4s^4}, \quad A \sim \frac{1}{2s^2}, \tag{C4}$$

while for $s \to 0$,

$$I \sim \begin{cases} -\log s, & \gamma = 0, \\ \dfrac{1}{\gamma s^\gamma}, & 0 < \gamma \leq 2 \end{cases} \tag{C5}$$

and

$$A \sim \begin{cases} \dfrac{1}{(3-\gamma)(2-\gamma)}, & 0 \leq \gamma < 2, \\ -\log s, & \gamma = 2. \end{cases} \tag{C6}$$

This paper has been typeset from a TEX/LATEX file prepared by the author.